Laser-Chirp Controlled Terahertz Wave Generation from Air Plasma

Xing Xu(徐行)[1,2,3,4†], Yindong Huang(黄崟东)[2†*], Zhelin Zhang(张喆林)[5,6,7†], Jinlei Liu(刘金磊)[8], Jing Lou(娄菁)[2], Mingxin Gao(高明鑫)[2], Shiyou Wu(吴世有)[1,3,4], Guangyou Fang(方广有)[1,3,4], Zengxiu Zhao(赵增秀)[8], Yanping Chen(陈燕萍)[6,7*], Zhengming Sheng(盛政明)[5,6,7], and Chao Chang(常超)[1,2*]

[1]*Aerospace Information Research Institute, Chinese Academy of Sciences, Beijing 100094, China*
[2]*Innovation Laboratory of Terahertz Biophysics, National Innovation Institute of Defense Technology, Beijing 100071, China*
[3]*Key Laboratory of Electromagnetic Radiation and Sensing Technology, Chinese Academy of Sciences, Beijing 100190, China*
[4]*School of Electronic, Electrical and Communication Engineering, University of Chinese Academy of Sciences, Beijing 100049, China*
[5]*Tsung-Dao Lee Institute, Shanghai Jiao Tong University, Shanghai 200240, China*
[6]*Key Laboratory for Laser Plasmas, School of Physics and Astronomy, Shanghai Jiao Tong University, Shanghai 200240, China*
[7]*Collaborative Innovation Center of IFSA, Shanghai Jiao Tong University, Shanghai 200240, China*
[8]*Department of Physics, College of Sciences, National University of Defense Technology, Changsha 410073, China*

(Received 17 February 2023; accepted manuscript online 22 March 2023)

We report the laser-chirp controlled terahertz (THz) wave generation from two-color-laser-induced air plasma. Our experimental results reveal that the THz wave is affected by both the laser energy and chirp, leading to radiation minima that can be quantitatively reconstructed using the linear-dipole-array model. The phase difference between the two colors, determined by the chirp and intensity of the laser, can account for the radiation minima. Furthermore, we observe an asynchronous variation in the generated THz spectrum, which suggests a THz frequency-dependent phase matching between the laser pulse and THz wave. These results highlight the importance of laser chirp during the THz wave generation and demonstrate the possibility of modulating the THz yields and spectrum through chirping the incident laser pulse. This work can provide valuable insights into the mechanism of plasma-based THz wave generation and offer a unique means to control THz emissions.

DOI: 10.1088/0256-307X/40/4/045201

Two-color-laser-induced air plasma is a promising method for generating ultra-broad and coherent terahertz (THz) radiation,[1] with numerous applications in remote sensing, ultrafast control, nonlinear modulation, and bio-detection.[2–6] In order to optimize the THz yield, several attempts have been made, including laser polarization control,[7,8] phase delay variation between the two-color laser fields,[9,10] alteration of the driven wavelength,[3,11–13] gas media type modification,[14] and adding an additional DC field.[15,16] To engineer and optimize the THz radiation, it is crucial to understand the generation mechanism. The four-wave mixing model[9] and the photo-current model[17] were initially proposed to explain the THz wave generation (TWG), both of which showed strong dependence on the relative phase between the two colors. However, recent research has updated these concepts. It is appeared that four-wave mixing from the laser exposed neutrals is primarily responsible for the higher frequency components of the THz outputs, whereas TWG at lower frequency is more closely associated with plasma properties.[18] Research from various groups has reported a strong correlation between plasma frequency and spectral peak of THz waves.[18–21] Additionally, laser induced air plasma has also been found to exhibit plasma frequency-dependent broadband absorption in the THz band.[22,23]

The plasma effect on TWG is not limited in the peak frequency of THz emissions. When the laser is powerful enough to create a long plasma filament, localized radiative dipole will exhibit an ω–2ω walk-off that varies with the laser's propagation distance along the filament.[24,25] THz emission can be modulated through the coherent summation of these localized radiative dipoles.[26–29] Chirping the laser pulse has been shown to optimize THz energy yield in air plasma,[30–32] as well as in crystals such as lithium niobate.[33,34] Unlike the 'quasi-free' electron in a strong laser field that exhibits chirp-dependent ionization rate and kinetic energy,[35,36] THz yield from air plasma is sensitive to the chirp-dependent temporal overlap of the incident two colors, particularly for an incident laser with a short pulse duration.[31,32] Therefore, chirping laser pulses can be used to optimize and modulate the THz wave. How-

†X. Xu, Y. Huang, and Z. Zhang contributed equally to this work.
*Corresponding authors. Email: yindonghuang@nudt.edu.cn; yanping.chen@sjtu.edu.cn; gwyzlzssb@pku.edu.cn
© 2023 Chinese Physical Society and IOP Publishing Ltd

ever, such modulation relies on a thorough understanding of the dynamics involved.

In this Letter, we demonstrate the manipulation of THz emission yield and spectrum by controlling the chirp and energy of the incident laser pulse. Experimental results reveal that, as laser energy increases, the peak-to-peak amplitude of the THz wave exhibits a significant yield minimum, which corresponds to the phase inversion of the THz waveform and can be modulated by laser chirp. By applying the linear dipole array (LDA) model,[25] we can quantitatively reconstruct these THz intensity minima. The reversal of the THz waveform around the intensity minimum suggests that the evolution of the relative phase between the two-color laser pulses along the filament leads to the coherent elimination of THz yield, attributed to the ω–2ω walk-off of the chirped pulse introduced by the group velocity mismatch (GVM) of the frequency-doubling crystal. Additionally, THz frequency-dependent spectrum evolution with the laser energy is demonstrated, showing the ability to control the emission spectrum. Our results contribute to a deeper understanding of the coherence properties of localized dipoles for THz emissions and can benefit the plasma-based THz technology.

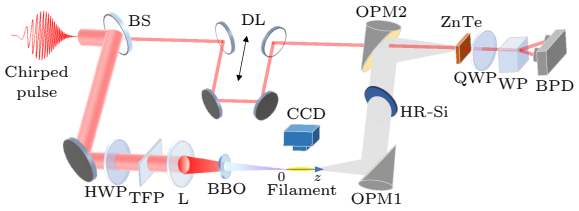

Fig. 1. Schematic presentation of the experimental setup. BS, beam splitter; DL, delay line; HWP, half-wave plate; TFP, thin film polarizer; L, lens; BBO, type-I β-barium borate crystal; OPM1 and OPM2, off-axis parabolic mirrors; HR-Si, high-resistivity silicon plate; QWP, quarter-wave plate; WP, Wollaston prism; BPD, balanced photodiodes.

Experimentally, the laser pulse with a central wavelength of 800 nm and a repetition rate of 1 kHz was focused by an $f = 30$ cm plano-convex lens to form a filament in ambient air, as shown in Fig. 1. The chirp of the laser pulse could be controlled by tuning the distance between the compressor diffraction gratings. A 0.1-mm-thick type-I β-barium borate (β-BBO) crystal was used to generate the second harmonic (SH) wave before the laser pulse underwent filamentation. The crystal ordinary axis for the fundamental wave (FW) was tuned to be about 56° with respect to the p-polarized FW field. The frequency doubling efficiency depends on the laser energy and pulse duration, whose maximum value is ∼15%. The distance from the β-BBO crystal to the focal point was chosen to optimize the THz yield.[37] With a charge-coupled device (CCD) camera arranged on a stereomicroscope, the fluorescence of filament was measured to estimate the plasma density simultaneously. THz emission from the filament was collected by a pair of off-axis parabolic mirrors and detected by the electro-optic sampling technique with a 2-mm-thick ZnTe crystal.

To characterize the chirp degree of the incident laser pulse, we use a dimensionless chirp parameter β defined as[35]

$$\beta \triangleq \sqrt{(\tau_{\rm p}/\tau_0)^2 - 1}, \tag{1}$$

where $\tau_{\rm p}$ is the pulse duration of the chirped pulse and $\tau_0 = 99$ fs is the Fourier-limited pulse duration ($\beta = 0$). The laser pulse duration was measured by a femtosecond autocorrelator. In addition to the Fourier-transform-limited laser pulse, we also calibrated the positive chirped pulse with pulse durations of 102 fs, 108 fs, 123 fs, and 138 fs ($\beta = 0.25$, 0.44, 0.74, and 0.97), respectively. A larger value of β results in a wider pulse duration. As reported in Refs. [38,39], the pulse-duration-dependent THz yield is primarily due to the ionization during the filamentation process. However, in our experiments, varying the pulse duration did not significantly alter the intensity and distribution of the fluorescence signal (see Fig. S4 in the Supplementary Material), suggesting that pulse duration is not the main factor affecting THz yield minima.

Previous studies by different groups have reported chirp-dependent THz generation, while their results appear to be dependent on laser energy.[30,31,40,41] In this study, we conducted a systematic measurement of laser chirp- and energy-dependent THz waveforms, as shown in Fig. 2(a). Each vertical line corresponds to a THz waveform at a specific incident laser energy. The extracted peak-to-peak THz amplitudes $A_{\rm THz}$ of the THz waveforms are shown by red stars in Fig. 2(c). When the laser is Fourier-transform-limited ($\beta = 0$), the amplitude of the THz wave increases monotonically with the laser energy. However, for a chirped pulse with $\beta = 0.25$, 0.44, 0.74, and 0.97, the THz waveform will exhibit a more complex relationship with laser energy. As seen in Fig. 2(a), the measured THz waveform undergoes a phase inversion as laser energy increases. At the same time, the THz amplitude $A_{\rm THz}$ in Fig. 2(c) shows a minimum around the phase-reversing points of the incident laser energy.

The one-dimensional LDA model[25] is applied to understand the observed results. The details of the model can be found in the Supplementary Material. The simulated THz waveform from the filament versus the laser energy for different chirp parameters are shown in Fig. 2(b). The corresponding THz peak-to-peak amplitudes are given by the blue lines in Fig. 2(c). All the simulation results are in good agreements with the experimental data. The main concept of the LDA model is that the THz radiation is regarded as a coherent superposition of the THz wave emitted from each dipole located along the filament. The coherent property of the localized plasma sheets along the filament can be revealed by the modulation of THz waves via the ω–2ω walk-off of the incident lasers, e.g., introducing from the length of plasma filament[24,28] and the phase delay between the two colors.[29,42] Therefore, it is necessary to reconstruct the evolution of relative phase difference between the two colors.

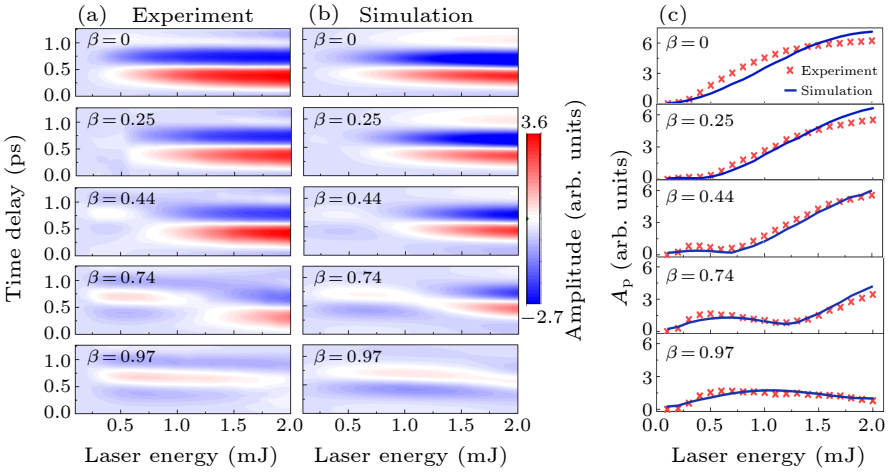

Fig. 2. (a) The measured THz waveforms vs the laser energy with the chirp parameter of 0, 0.25, 0.44, 0.74, and 0.97. (b) The corresponding simulation results. (c) Laser energy- and chirp-dependent THz peak-to-peak amplitudes (A_p). The red stars show the experimental data, and the solid blue line is the corresponding simulation result.

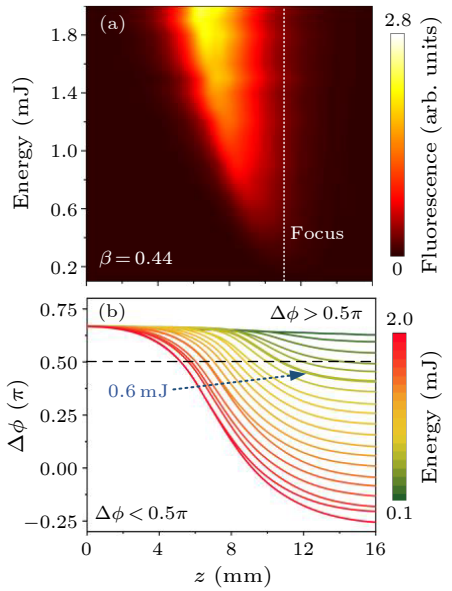

Fig. 3. A specific case of $\beta = 0.44$. (a) Fluorescence of the filament along z axis at different laser energies. The white dotted line points out the geometric focus of the light path. (b) Calculated relative phase between the two-color laser components while propagating in the plasma filament. The black dashed line indicates the case of $\Delta\phi = 0.5\pi$.

The electric field of the FW with a Gaussian shape can be expressed as $E_\omega(t) = E_p g_1(t)\cos(\phi_1(t))$, where E_p is the peak amplitude, $g_1(t) = \exp(-2\ln 2 t^2/\tau_p^2)$ indicates the pulse envelope, and $\phi_1(t) = \omega_0 t + [2\ln 2/(\beta + 1/\beta)](t^2/\tau_0^2)$ represents the phase term that laser frequency drifts linearly in time. Here, ω_0 is the fundamental frequency, β is the chirp parameter and τ_p is the pulse duration. The corresponding SH laser pulse can be expressed as $E_{2\omega(t)} = E_2 g_2(t)\cos[\phi_2(t)]$, with $g_2(t) = g_1[\sqrt{2}(t - \tau_d)]$ and $\phi_2(t) = \phi_0(\beta) + 2\phi_1(t - \tau_d)$.[43] E_2 is the SH peak amplitude, which depends on the laser chirp and energy, $g_2(t)$ is the Gaussian envelope, $\phi_2(t)$ is the SH phase, and $\phi_0(\beta)$ is the initial SH phase originating from the group phase mismatch in the BBO crystal. The time delay τ_d is introduced by group dispersion between the FW and SH from air and filament, defined as $\tau_d = \Delta n_a d/c + \Delta n_f z/c$, where c is the speed of light in vacuum, and Δn is the refractive index difference between the FW and SH. We use the subscript notations a and f to distinguish the parameters in air and filament. Then, we obtain the relative phase difference between the two colors, which reads

$$\Delta\phi = \phi_1(t) - \frac{1}{2}\phi_2(t) \approx \omega_0\tau_d - \frac{1}{2}\phi_0(\beta), \tag{2}$$

with $\tau_d \ll \tau_0$. The relative phase distribution along the filament originates from three parts, which can be expressed as

$$\Delta\phi(d, z, \beta) = \phi_a(d) + \phi_f(z) - \frac{1}{2}\phi_0(\beta), \tag{3}$$

where $\phi_a(d) = \omega_0\Delta n_a d/c$ is the phase accumulated in air, $\phi_f(z) = \omega_0\Delta n_f z/c$ is the phase in filament, and $\phi_0(\beta)$ is the phase introduced by the BBO crystal. $\Delta\phi$ is applied to calculate the drift motion of the ionized electrons, which leads to the spatial charge separation between the electrons and the left ions. The influence of the chirp on $\Delta\phi$ mainly stems from $\phi_0(\beta)$.

Based on the LDA model, we will present the reconstructed phase difference between the two colors. As an example, the fluorescence intensities and phase variations under different incident laser energies with the chirp parameter $\beta = 0.44$ are shown in detail in Fig. 3. The distance d between the BBO crystal and the original point of z was measured to be 23.47 cm, which can be used to calculate ϕ_a. Meanwhile, for a fixed chirp parameter, ϕ_0 is constant. To give a quantitative description of the plasma, we present the CCD-obtained fluorescence of the filament along the z axis in Fig. 3(a). It can be observed from Fig. 3(a) that, as the laser energy increases, the starting point of the filament moves forward roughly by a distance of 6 mm. This distance is much smaller than the Rayleigh length of the focusing THz spot, which means that the field strength of the THz wave does not change significantly with the moving focal plane. In other words, as

mentioned in Ref. [44], the detected THz wave will only endure a phase shift of the THz waveform due to Gouy phase shift of the focusing THz wave. Along the propagation distance z of the filament, the electron densities of the local plasma sheets directly affect the refractive indexes of the two colors, which makes the phase difference ϕ_f a function of the distance z and the input laser energies.

Then, by fitting a suitable initial phase $(\phi_a+\phi_0)$ at $z = 0$ to reproduce the experimentally observed THz emission, the relative phase distribution $\Delta\phi$ can be calculated,[25] as shown in Fig. 3(b). Note that the values of $\cos(\Delta\phi)$ on both sides of the dividing line of $\Delta\phi = 0.5\ \pi$ take the opposite signs, resulting in a contrary polarity of the dipoles. The highlighted evolution curve indicates the 0.6 mJ case, which is located at the phase-turning regions of the case $\beta = 0.44$ in Fig. 2(c). In that case, it shows a relative equivalent distribution of the opposite-oscillating localized contributions to the coherent summation of THz outputs, explaining why the total THz radiation vanishes and A_{THz} presents a minimum. For the negatively chirp laser, the laser-energy dependent THz output does not exhibit any emission minimum within the energy range of input laser. This is because the filament length required for changing the polarity between the adjacent dipoles will be much longer than the length for positive chirps when the laser chirp parameter is negative or zero. However, the length of the filament (oscillating dipoles) is limited by the laser energy in our experiment.

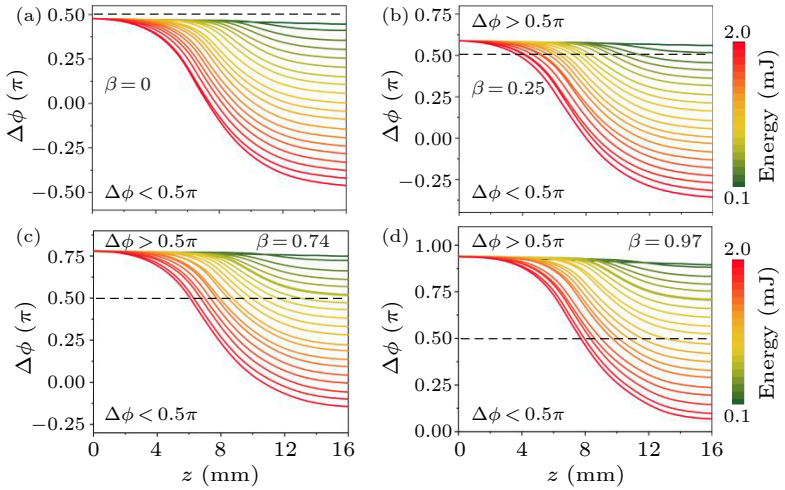

Fig. 4. Calculated relative phase between the two-color laser components while propagating in the plasma filament, for $\beta = 0$ (a), 0.25 (b), 0.74 (c), and 0.97 (d).

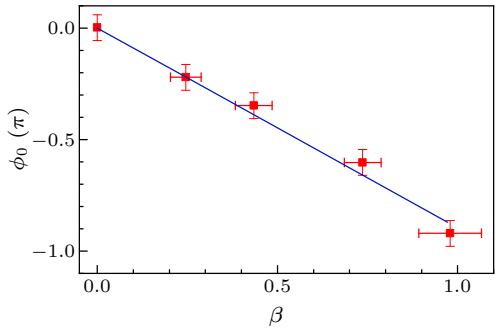

Fig. 5. Behavior of ϕ_0 with the chirp parameter. The red solid points and the blue line indicate the experimental data with error bars and the fitting function, respectively.

When the chirp of the incident laser pulse changes, the phase term ϕ_0 varies and affects the total relative phase $\Delta\phi$, resulting in a shift of the energy-dependent emission minima shown in Fig. 2(c). To better present the results, we also provide the reconstructed relative phase variation of other chirp parameters β for comparison, as shown in Fig. 4. Based on the reconstructed evolution of $\Delta\phi$, we can find a linear relationship between ϕ_0 and β, as shown in Fig. 5. This result indicates a chirp-dependent phase difference within the frequency doubling process. In our experiment, the GVM of the BBO crystal induces a time domain walk-off of the two colors, making the SH pulse propagate more slowly than the FW pulse. Due to the thin BBO crystal used in our experiment, the GVM is too small to change the intensity of SH generation. However, for the relative-phase sensitive TWG,[45] the temporal walk-off of the two colors determines the relative phase $\Delta\phi$, thus can control the conversion efficiency.[31]

Furthermore, the influence of chirp on THz generation is not limited to the temporal walk-off of the incident two colors, but also affects the THz spectra due to phase-matching. Take $\beta = 0.44$ as an example, the phase reversal of the THz waveform can be clearly seen in Fig. 6(a) when the laser energy is between 0.4 mJ and 0.8 mJ. Note that, although A_p has a yield minimum as the laser energy increases in Fig. 2(c), its intensity cannot be reduced to zero, indicating an asynchronous variation of the generated THz spectrum. The corresponding spectrum of the THz waveforms is presented in Fig. 6(b) to illustrate the asynchronous variation of THz spectrum. The trends of variations of THz amplitudes can be divided to the high-frequency (HF) part, which mainly corresponds to frequencies ranging from 1.5 to 2.5 THz, and the low-frequency (LF) part corresponding to 0.5–1.2 THz (with a peak at about 0.9 THz).

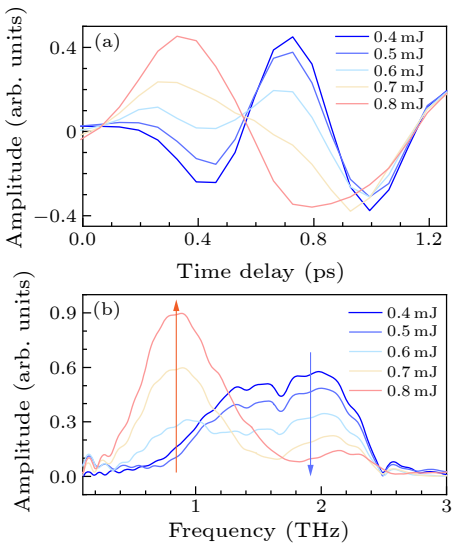

Fig. 6. The phase-reversing transition process of the THz wave in the case of $\beta = 0.44$. (a) The THz waveforms under the laser energy from 0.4 mJ to 0.8 mJ. (b) The corresponding THz spectrum.

The different behaviors between the HF and LF parts can be roughly understood by considering the phase matching conditions between the THz emission from localized dipoles and the incident laser. For simplicity, the air plasma is treated as a cylindrical uniform gaseous filament with the plasma frequency $\omega_{\rm p}$, and the refractive index will be modified by a resonant absorption centered at $\omega_{\rm p}/\sqrt{2}$.[22,23] Therefore, the refractive-index difference $\Delta n'$ between the FW and THz waves can be written as

$$\Delta n' = n_{\omega_0} - n_{\Omega} \simeq 1 - \left(\sqrt{1 - \frac{\omega_{\rm p}^2}{\Omega^2 - \omega_{\rm p}^2/2 + i\Gamma\Omega}}\right)_{\rm Re}, \quad (4)$$

where ω_0 indicates the 800 nm pulse, Ω is the THz frequency, $\omega_{\rm p}$ is the plasma frequency, and Γ is the collision frequency. Then, the coherent buildup length $L_{\rm c}$ can be expressed as

$$L_{\rm c}(\Omega) = \frac{2\pi c}{\Delta n' \Omega}. \quad (5)$$

Considering a typical condition of air plasma such that $\omega_{\rm p} \sim 1$ THz and $\Gamma \sim 0.5$ THz, the calculated $L_{\rm c}$ peaks at 0.85 THz with an estimated value of 2.75 cm. For 0.9 THz, $L_{\rm c}$ is 0.5 cm, while the value of $L_{\rm c}$ for 1.8 THz is only 0.1 cm. Based on these estimations, when the length of filament exceeds the coherent buildup length of the HFs of THz wave, the LF part of the THz frequencies will maintain a buildup generation, while the HF part of THz wave will undergo a coherent suppression of the output. The turning point of the coherent suppression is jointly determined by the initial phase of the localized dipoles and the filament length. At the same incident energy, chirping the laser pulse does not significantly change the filament length and fluorescence (see the Supplementary Material for details). However, as shown in Fig. 6, chirping the laser will introduce a phase shift between the two colors, which manipulates the initial phase of the dipoles along the filament. Meanwhile, the phase mismatch between the THz wave and laser will lead to an asynchronous variation of the generating spectrum, emphasizing the plasma effect on the prorogation of THz wave. This asynchronous variation of the generating spectrum, reflecting the differences in phase matching at different frequencies, can be used to modulate the central frequency of THz radiation. In addition, it is worth noting that the coherence buildup length strongly depends on the collision frequency of the plasma, suggesting the need for careful characterization of the collision and relaxation within the filament for optimizing and controlling the plasma-based THz generation.

In summary, we have thoroughly investigated the laser chirp dependence of the TWG from the two-color laser induced filament. By varying the chirp and laser intensity, we are able to identify and control the radiation minima, demonstrating the coherent properties of localized THz emitters. Quantitatively agreement is achieved between the experimental results and the LDA-model-based simulations. We find an additional phase ϕ_0 that is proportional to the chirp parameter, induced by the frequency doubling crystal. The phase matching between the laser pulse and the THz wave is also analyzed to understand the asynchronous variation of the generating spectrum.

Our findings provide a unique opportunity to manipulate the THz energy yield and output spectrum by adjusting the laser chirp parameters. Other fields of research, such as the near-field THz microscopy[46] and remote sensing,[47] which utilize optically induced plasma, can benefit from our results. Furthermore, in recent years, filament-based THz sources have been extensively studied using the long-wave infrared[3,11–14] and other frequency ratios.[48,49] Although the present LDA model only deals with the THz wave generation from near-infrared two-color fields (800 nm + 400 nm), it may be possible to extend to other wavelengths for a better understanding of wavelength-dependent THz emission by incorporating electronic dynamics into dynamics of local dipoles, e.g., avalanche ionization,[50] many-body effects,[51] and trapping of excited states.[13]

Acknowledgments. This work was supported by the National Natural Science Foundation of China (Grant Nos. 12174449, 12225511, T2241002, 12074250, 11991073, 12135009, 61988102, and 61971397), the National Key Research and Development Program of China (Grant Nos. 2019YFA0307703 and 2018YFB2202500). C.C. acknowledges the support from the XPLORER PRIZE. Y.H. thank Yutong Li and Xiaowei Wang for helpful discussions.

References

[1] Cook D J and Hochstrasser R M 2000 *Opt. Lett.* **25** 1210
[2] Liu J L, Dai J M, Chin S L, and Zhang X C 2010 *Nat. Photon.* **4** 627
[3] Koulouklidis A D, Gollner C, Shumakova V, Fedorov V Y, Pugžlys A, Baltuška A, and Tzortzakis S 2020 *Nat. Commun.* **11** 292
[4] Xu K Y, Liu M K, and Arbab M H 2022 *Appl. Phys. Lett.* **120** 181107
[5] Markelz A G and Mittleman D M 2022 *ACS Photon.* **9** 1117
[6] Lou J, Jiao Y, Yang R, Huang Y, Xu X, Zhang L, Ma Z, Yu Y, Peng W, Yuan Y, Zhong Y, Li S, Yan Y, Zhang F,

Liang J, Du X, Chang C, and Qiu C W 2022 *Proc. Natl. Acad. Sci. USA* **119** e2209218119
[7] Meng C, Chen W, Wang X, Lu Z, Huang Y, Liu J, Zhang D, Zhao Z, and Yuan J 2016 *Appl. Phys. Lett.* **109** 131105
[8] Zhang Z L, Chen Y P, Cui S, He F, Chen M, Zhang Z, Yu J, Chen L, Sheng Z, and Zhang J 2018 *Nat. Photon.* **12** 554
[9] Xie X, Dai J, and Zhang X C 2006 *Phys. Rev. Lett.* **96** 075005
[10] Kim K Y 2009 *Phys. Plasmas* **16** 056706
[11] Nguyen A, Kaltenecker K J, Delagnes J C, Zhou B, Cormier É, Fedorov N, Bouillaud R, Descamps D, Thiele I, Skupin S, Jepsen P U, and Bergé L 2019 *Opt. Lett.* **44** 1488
[12] Jang D, Schwartz R M, Woodbury D, Griff-McMahon J, Younis A H, Milchberg H M, and Kim K Y 2019 *Optica* **6** 1338
[13] Yu Z, Sun L, Zhang N, Wang J, Qi P, Guo L, Sun Q, Liu W, and Misawa H 2022 *Ultrafast Sci.* **2022** Article ID 9853053
[14] Zhao H, Zhang L, Huang S, Zhang S, and Zhang C 2018 *IEEE Trans. THz Sci. Technol.* **8** 299
[15] Wang T J, Marceau C, Chen Y, Yuan S, Thberge F, Chteauneuf M, Dubois J, and Chin S L 2010 *Appl. Phys. Lett.* **96** 211113
[16] Liu Y, Liu S, Houard A, Mysyrowicz A, and Tikhonchuk V T 2020 *Chin. Phys. Lett.* **37** 065201
[17] Kim K Y, Taylor A J, Glownia J H, and Rodriguez G 2008 *Nat. Photon.* **2** 605
[18] Andreeva V A, Kosareva O G, Panov N A, Shipilo D E, Solyankin P M, Esaulkov M N, de González A M P, Shkurinov A P, Makarov V A, Bergé L, and Chin S L 2016 *Phys. Rev. Lett.* **116** 063902
[19] Debayle A, Gremillet L, Bergé L, and Köhler C 2014 *Opt. Express* **22** 13691
[20] Li N, Bai Y, Miao T, Liu P, Li R, and Xu Z 2016 *Opt. Express* **24** 23009
[21] Li X L, Bai Y, Li N, and Liu P 2018 *Opt. Lett.* **43** 114
[22] Zheng Z G, Huang Y D, Guo Q *et al.* 2017 *Phys. Plasmas* **24** 103303
[23] Huang Y D, Xiang Z X, Xu X *et al.* 2021 *Phys. Rev. A* **103** 033109
[24] You Y S, Oh T I, and Kim K Y 2012 *Phys. Rev. Lett.* **109** 183902
[25] Zhang Z L, Chen Y P, Chen M, Zhang Z, Yu J, Sheng Z M, and Zhang J 2016 *Phys. Rev. Lett.* **117** 243901
[26] Liu Y, Houard A, Durand M, Prade B, and Mysyrowicz A 2009 *Opt. Express* **17** 11480
[27] Meng C, Lu Z, Huang Y, Wang X, Chen W, Zhang D, Zhao Z, and Yuan J 2016 *Opt. Express* **24** 12301
[28] Panov N A, Kosareva O G, Andreeva V A, SavelEv A B, and Shkurinov A P 2011 *JETP Lett.* **93** 638
[29] Chen G, Teramoto T, and Tonouchi M 2021 *J. Infrared Millimeter Terahertz Waves* **42** 647
[30] Nguyen A, de Alaiza M P G, Thiele I, Skupin S, and Bergé L 2018 *New J. Phys.* **20** 033026
[31] Zhang Z, Panov N, Andreeva V, Zhang Z, Slepkov A, Shipilo D, Thomson M D, Wang T J, Babushkin I, Demircan A, Morgner U, Chen Y, Kosareva O, and Savel'ev A 2018 *Appl. Phys. Lett.* **113** 241103
[32] Yu Z, Zhang N, Wang J, Dai Z, Gong C, Lin L, Guo L, and Liu W 2022 *Opto-Electron. Adv.* **5** 210065
[33] Jolly S W, Matlis N H, Ahr F, Leroux V, Eichner T, Calendron A L, Ishizuki H, Taira T, Kärtner F X, and Maier A R 2019 *Nat. Commun.* **10** 2591
[34] Zhang B, Ma Z, Ma J, Wu X, Ouyang C, Kong D, Hong T, Wang X, Yang P, Chen L, Li Y, and Zhang J 2021 *Laser Photon. Rev.* **15** 2000295
[35] Saalmann U, Giri S K, and Rost J M 2018 *Phys. Rev. Lett.* **121** 153203
[36] Luo S, Liu J, Li X *et al.* 2021 *Phys. Rev. Lett.* **126** 103202
[37] Kim K Y, Glownia J H, Taylor A J, and Rodriguez G 2007 *Opt. Express* **15** 4577
[38] Dai H and Liu J 2011 *J. Mod. Opt.* **58** 859
[39] Lu C, He T, Zhang L, Zhang H, Yao Y, Li S, and Zhang S 2015 *Phys. Rev. A* **92** 063850
[40] Wang T J, Chen Y, Marceau C, Theberge F, Chateauneuf M, Dubois J, and Chin S L 2009 *Appl. Phys. Lett.* **95** 131108
[41] Wang T J, Yuan S, Chen Y, Daigle J F, Marceau C, Theberge F, Chateauneuf M, Dubois J, and Chin S L 2010 *Appl. Phys. Lett.* **97** 111108
[42] Wang T J, Ju J, Wei Y, Li R, Xu Z, and Chin S L 2014 *Appl. Phys. Lett.* **105** 051101
[43] Silaev A A, Romanov A A, and Vvedenskii N V 2020 *Opt. Lett.* **45** 4527
[44] Zhao J, Zhang Y, Wang Z, Chu W, Zeng B, Liu W, Cheng Y, and Xu Z 2014 *Laser Phys. Lett.* **11** 095302
[45] Mi Y, Johnston K, Shumakova V, Møller S H, Jana K, Zhang C, Staudte A, Sederberg S, and Corkum P B 2022 *Photon. Res.* **10** 96
[46] Wang X K, Ye J S, Sun W F, Han P, Hou L, and Zhang Y 2022 *Light Sci. Appl.* **11** 129
[47] Qi P, Qian W, Guo L, Xue J, Zhang N, Wang Y, Zhang Z, Zhang Z, Lin L, Sun C, Zhu L, and Liu W 2022 *Sensors* **22** 7076
[48] Kostin V A, Laryushin I, Silaev A A, and Vvedenskii N V 2016 *Phys. Rev. Lett.* **117** 035003
[49] Zhang L L, Wang W M, Wu T, Zhang R, Zhang S, Zhang C, Zhang Y, Sheng Z, and Zhang X 2017 *Phys. Rev. Lett.* **119** 235001
[50] Woodbury D, Goffin A, Schwartz R M, Isaacs J, and Milchberg H M 2020 *Phys. Rev. Lett.* **125** 133201
[51] Schuh K, Kolesik M, Wright E M, Moloney J V, and Koch S W 2017 *Phys. Rev. Lett.* **118** 063901